AN ABSTRACT OF THE THESIS OF

SOMPONG VONGSURI _ for the _ M. S. _ in Mechanical Engineering
     (Name)   (Degree)   (Major)

Date thesis is presented _ _ _July 16, 1965 _ _ _ _ _ _ _

Title _ AN INVESTIGATION OF HEAT TRANSFER AND PRESSURE

_ DROP ACROSS A FROSTED FINNED COIL

Abstract approved ███████████████████████████
(Major Professor)

The formation of frost on a forced convection refrigeration coil, operating below the freezing temperature is known to have the effect of imparing the efficiency of a refrigeration system. This investigation was directed toward the study of the behavior of the overall coefficient of heat transfer and the air static pressure drop for a frosted coil.

The experiment was conducted with a finned tube coil having staggered tube arrangement. The experimental equipment was so designed that the frost accumulation on the test coil could be measured with a platform scale. A chilled solution of 30 percent by weight of ethylene glycol and water supplied the cooling for the test coil. Tests were run at constant air flow rates of 585, 685 and 775 CFM. In each test the inlet air was maintained approximately at 32° F with a specific humidity of 0. 003 lbs of moisture per lb of dry

air; the supplied antifreeze solution was kept at about 14° F with a flow rate of 1, 853 lbs per hr. Sufficient data were recorded, during each test, to determine the overall coefficient of heat transfer and the air static pressure drop through the test coil at various frost accumulations.

It was observed that the overall coefficient of heat transfer at constant air flow rate increased slightly as frost first accumulated on the test coil and then decreased after the peak had been reached as the frost continued to increase. The air pressure drop increased continuously with increasing frost accumulation on the test coil. For each increment of frost weight per square foot of coil surface the magnitude of the air pressure drop was found to be greater at the higher air flow rates. The agreement between the results of the present investigation and the one previously made on the coils having in-line tubes arrangement suggested that the behavior of the overall coefficient of heat transfer and the air pressure drop were independent of coil geometry. For a system with a fixed capacity and design conditions the decrease in overall coefficient of heat transfer, during the heavy frosting, would lower the system efficiency by the reduction in the coefficient of performance of the refrigeration system. The increase in pressure drop at increasing frost accumulation on the coil surface would have a direct effect on lowering the system capacity by reducing the air flow in the system.

The limited information made available by this investigation was not enough to cover the wide range of operating conditions and heat exchangers encountered in practice. More extensive research would be necessary to provide sufficient information for a better design of the refrigeration systems when the formation of frost on the heat exchanger surface could not be avoided.

AN INVESTIGATION OF HEAT TRANSFER
AND PRESSURE DROP ACROSS A FROSTED FINNED COIL

by

SOMPONG VONGSURI

A THESIS

submitted to

OREGON STATE UNIVERSITY

in partial fulfillment of
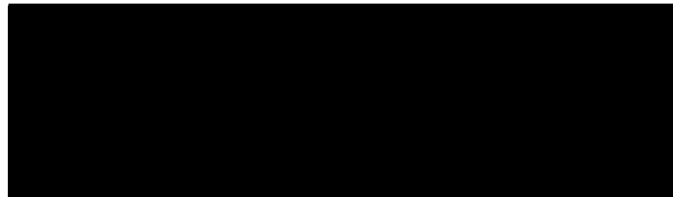the requirements for the
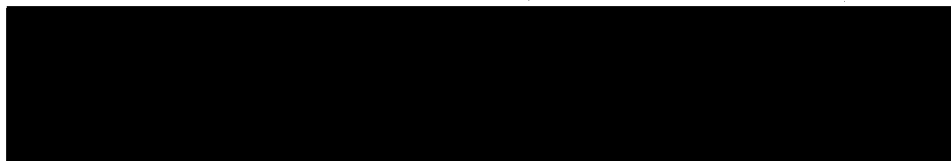degree of

MASTER OF SCIENCE

June 1966

APPROVED:

<div style="margin-left:2em">

████████████████████████████████

Professor of Mechanical Engineering

In Charge of Major

████████████████████

Head of Department of Mechanical and Industrial
Engineering

████████████████████████████████

Dean of Graduate School

</div>

Date thesis is presented   July 16, 1965

Typed by Nancy Kerley

ACKNOWLEDGEMENTS

TABLE OF CONTENTS

LIST OF FIGURES

LIST OF TABLES

NOMENCLATURE

A   Area, ft^2; A_a, total airside heat transfer area.

c_p Specific heat of air at constant pressure, Btu/lb-°F.

$\overset{o}{m}$ Flow rate, lb/min.

ΔP Air static pressure drop, inches of water.

t   Fluid temperature, °F.

t_w Wet-bulb temperatures of air, °F.

ΔT_m Logarithmic mean temperature difference, °F.

U   Overall coefficient of heat transfer, $Btu/hr-ft^2$-°F.

W   Specific humidity, lb of water vapor/lb dry air.

X   Frost intensity, grains of frost per ft^2 of total airside heat

        transfer area.

Subscripts

1   Entering conditions.

2   Leaving conditions.

a   Refers to air.

r   Refers to antifreeze.

m   Average condition.

AN INVESTIGATION OF HEAT TRANSFER
AND PRESSURE DROP ACROSS A FROSTED FINNED COIL

CHAPTER I

INTRODUCTION

Frost is encountered on an air cooling coil when the surface

temperature of the coil is below freezing and the air is cooled be-

low its dew point. This phenomenon is the result of both heat and

mass transfer. As the layer of frost increases, there is a corre-

sponding decrease in the performance of a cooling coil. To compen-

sate for this decreased performance of the system the design

engineer must design for a greater capacity. Unfortunately, little

information is available regarding the effect of frost formation on the

heat transfer coefficient and the pressure drop of the air flowing

across a cooling coil.

Stoecker (5) investigated the formation of frost on a refrigera-

tion coil by natural convection. He discovered that the heat transfer

coefficient increased as the formation of frost increased up to a

point after which it became nearly constant as the frost became

thicker. The initial increase in the heat transfer coefficient was due

to the roughening of the pipe surfaces which increased the turbulence

of the air flowing. There were two things which contributed to the

leveling off of the heat transfer coefficient. One was the increase

in external surface area and the other was the increase in thermal

conductivity of the denser frost as its thickness increased. In addi-

tion, he investigated the similar problem of forced convection across

finned tube coils (6). Throughout his tests the entering air condition

was kept constant at 32° F and 72 percent relative humidity. The

tests were run with various air velocities and at various accumula-

tions of frost. He concluded that with a constant air flow the over-

all coefficient of heat transfer for the coil first increased as frost

began to form and then decreased as frost thickened. The decrease

in the coefficient of heat transfer was, as he asserted, not of con-

cern in a refrigeration system. However, the reduction in air flow

that occurred due to frost formation lowered the capacity of the

system for the same refrigerant temperature, and hence served as

the best guide of the effect of frost on the coil performance. Beatty,

Finch and Schoeborn (1) investigated heat transfer to a tube under

frosting conditions, at approximately the freezing point of water,

by forced convection. Their results were quite similar to those

obtained by Stoecker. Chung and Algren (2) studied the frost forma-

tion and heat transfer on a cylindrical surface in humid air cross

flow under forced convection. Their studies were made to gain both

analytical and experimental insight into the performance of a frosted

evaporator coil. It was found that the density and thermal

conductivity as well as the frost thickness changed continuously as

frost was formed on the surface. A quasi-steady state was reached

when the effect of the increase in the frost thermal conductivity

nullified the effect of the increase in frost thickness. Other investi-

gators, such as Weber (7), Whitehurst (8), Lopper (3) and

Omelianchuk (4) also made extensive studies along these lines.

Their studies included forced and natural convection for other shapes

of heat transfer surfaces and various air flow patterns.

A. Objective

The objective of this thesis was to investigate the heat trans-

fer and pressure drop across a frosted finned coil by forced convec-

tion. This investigation differs from that of Stoecker (6) in two

aspects. First, the equipment was modified so that the weight of the

frost on the test coil could be measured by direct weighing without

removing the test coil. Secondly, the tube arrangement of the coil

was staggered rows of tubes.

B. Definitions and Terms

1. The definition of the overall coefficient of heat transfer U.

Throughout this investigation, the airside sensible heat trans-

fer was calculated by the formula

$$\overset{\circ}{Q} = 60 \, \overset{\circ}{m}_a \, c_p \, (t_{a_1} - t_{a_2}) \qquad (1)$$

where

$\overset{\circ}{Q}$ = Sensible heat transfer, Btu/hr.

$\overset{\circ}{m}_a$ = Mass rate of dry air flow, lb/min.

c_p = Specific heat of dry air, Btu/lb -°F.

t_{a_1} = Dry bulb temperature of air entering the test coil, °F.

t_{a_2} = Dry bulb temperature of air leaving the test coil, °F.

The overall coefficient of heat transfer, U, for the frost coil was

defined as

$$U = \frac{\overset{\circ}{Q}}{A_a \, \Delta T_m}$$

or

$$U = \frac{60 \, \overset{\circ}{m}_a \, c_p \, (t_{a_1} - t_{a_2})}{A_a \, \Delta T_m} \qquad (2)$$

U has the units of Btu per hr per ft^2 -°F and A_a is the total airside

heat transfer area of the coil in ft^2.

The term ΔT_m represents the logarithmic mean temperature

difference between the air and the coolant. Since the temperature

differences of the antifreeze circulated through the coil did not ex-

ceed 4° F, the logarithmic mean temperature difference between

the air and the antifreeze can be defined as

$$\Delta T_m = \frac{t_{a_1} - t_{a_2}}{\ln\left[\frac{t_{a_1} - t_r}{t_{a_2} - t_r}\right]} \qquad (3)$$

where

$$t_r = \frac{t_{r_1} + t_{r_2}}{2} \text{ represents the average antifreeze temperature,}$$

°F.

t_{r_1} = Temperature of the antifreeze entering the coil, °F.

t_{r_2} = Temperature of the antifreeze leaving the coil, °F.

By substituting equations (1) and (3) into (2), we obtain

$$U = \frac{60 \, \overset{\circ}{m}_a c_p}{A_a} \ln \frac{t_{a_1} - t_r}{t_{a_2} - t_r} \qquad (4)$$

It is evident that equation (4) gives the most compact formula for

calculating the overall coefficient of heat transfer.

2. The frost intensity X.

The weight of frost accumulated on the coil surface was

expressed in terms of frost intensity, X, which was defined as the

weight of frost per square foot of total airside heat transfer area.

The units of X were chosen to be grains of frost per ft^2 of airside

heat transfer area.

3. Pressure drop across the coil ΔP.

The data for pressure drop across the coil in inches of water at room temperature were converted to the corresponding values at 70° F. The following equations were used

$$(\rho \Delta P)_t = (\rho \Delta P)_{70} \qquad (5)$$

or

$$\Delta P_{70} = \frac{(\rho \Delta P)_t}{\rho_{70}} \text{ inches of } H_2O \text{ at } 70° F. \qquad (6)$$

where

t denotes room temperature, ° F; and

ρ denotes the density of water in lb_m/ft^3.

CHAPTER II

EXPERIMENTAL EQUIPMENT

Equipment and instrumentation were provided for measuring the heat transfer and pressure drop across the test coil. The test apparatus consisted of four major components: the air system, the test coil, the antifreeze system and the test station. The following sections will describe each of the major components separately.

A. The Air System

The air system was essentially a low-velocity closed circuit air duct. The air system and its components are shown in Figures 1 and 2. The air duct was made of No. 24 gauge galvanized steel, having 12 inch by 18 inch cross-section. Air flow was controlled by a manually operated louvered damper and circulated through the system by a 12-3/4 inch Viking blower, belt driven by a one third horse-power motor. The blower, motor and the damper were installed in an enclosed metal box integral to the air system. In order to measure the air flow in the system, an eight inch diameter orifice was installed in the supply duct at 11 feet from the blower discharge. The upstream and downstream static pressure taps were located at 12 inches and 6 inches respectively from the orifice. At each
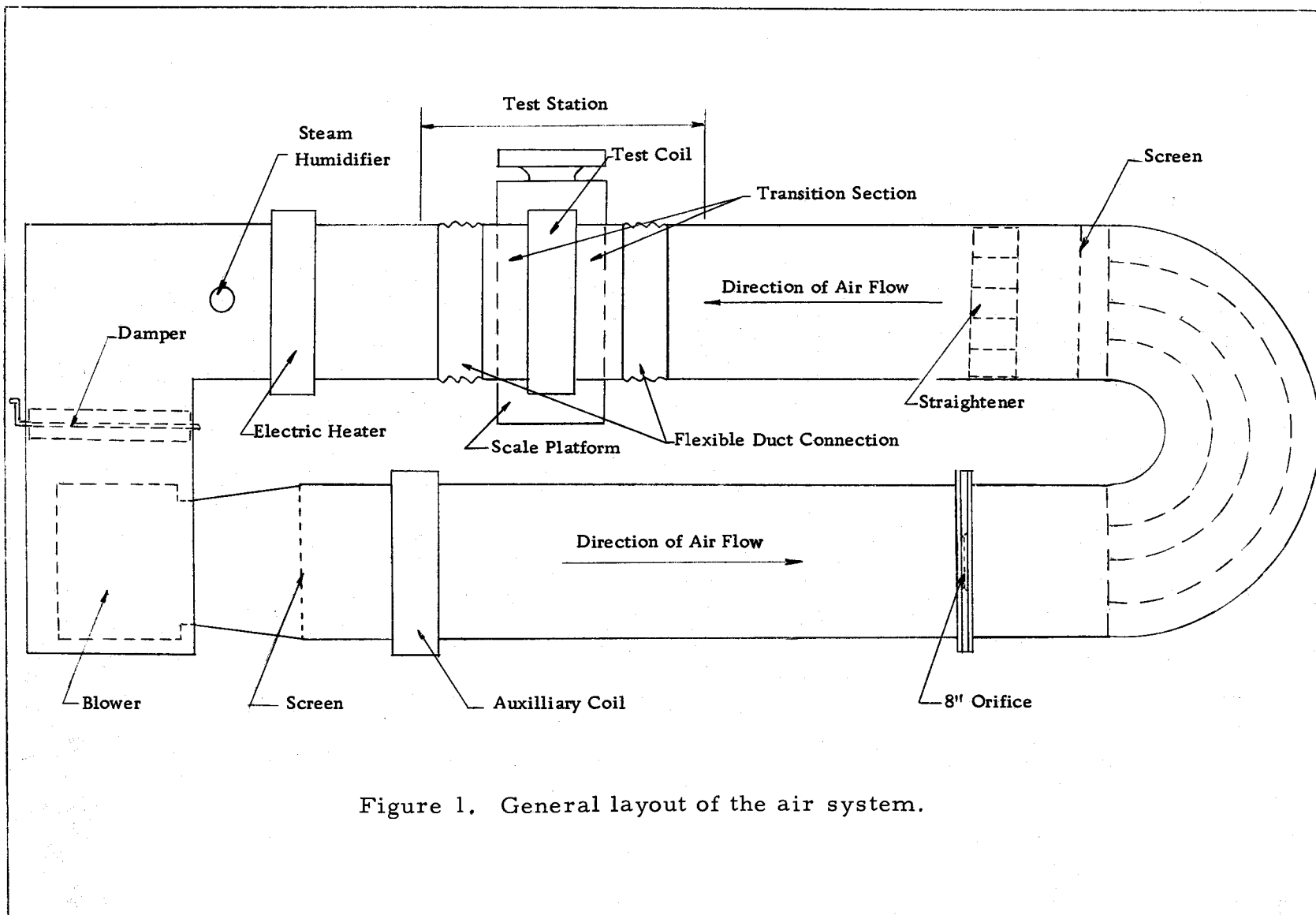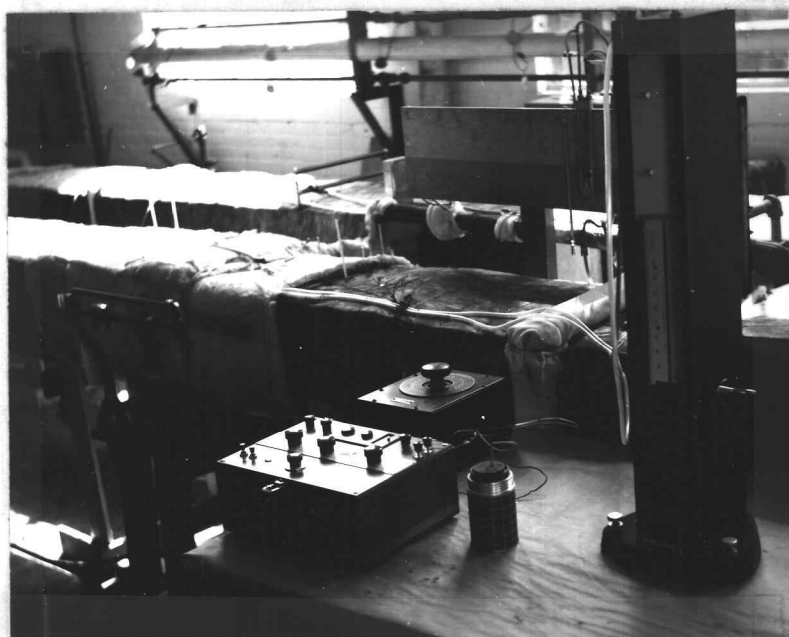
Figure 1. General layout of the air system.

(a)

(b)

Figure 2. Experimental apparatus.
(a) Insulated duct work.
(b) Temperature and pressure instrument.

location, there were four static pressure taps each located at the

center of the duct sides. The four pressure taps were connected

to a common 1/4 inch rubber tubing. The upstream and downstream

pressure taps were connected to a vertical water micro-manometer

which measured the pressure drop across the orifice. The water

micro-manometer had a maximum range of ten inches of water with

vernier scale reading to 0.001 inches of water; readings could be

further estimated to 0.0002 inches of water. The orifice was made

of 3/8 inch thick 15 inches by 21 inches aluminum plate bolted be-

tween the upstream and downstream duct flanges. It was calibrated

by pitot tube transverse method and the results are presented in

Figure 17 in the Appendix. The air flow was maintained constant in

the system by keeping a constant pressure drop across the orifice.

The test station was located preceeding the suction side of

the blower. It was so arranged that the temperature of air and anti-

freeze entering and leaving the test coil, together with the pressure

drop of the air and the frost weight on the test coil could be measured.

The detailed description of the test station is presented in a suc-

ceeding section.

A screen and a straightener were installed in the straight

duct section ahead of the test station to insure uniform air distribu-

tion entering the test coil.

The losses of heat and moisture from air to the test coil were

restored by an electric heater and a steam humidifier installed following the test station.

The electric heater had 3,000 watts total capacity at 115 volts a-c. It consisted of two 1,500 watts independent circuits. The first circuit was connected to a power-stat which allowed the control of input voltage from zero to 100 percent. The remaining circuit was direct connected to the power line through an on-off switch. With this arrangement, the two heater circuits were used to control the air temperature individually or simultaneously as desired.

The steam humidifier was made of a 3/4 inch steel pipe inserted vertically into the duct six inches downstream from the electric heater. Four 1/8-inch holes at one inch spacing from upper duct wall were drilled along the center line of the downstream face. The humidifier was supplied with five psig steam through a globe valve which was used to regulate the steam rate. In order to prevent steam from condensing inside the pipe, the dehumidifier pipe was completely insulated except at the openings. A valve was provided at the lower end of the humidifier pipe to drain the pipe.

An auxilliary cooling coil was installed downstream from the blower to cool air to the test condition initially. The antifreeze system and the auxilliary coil detail are presented in the succeeding sections.

All joints in the duct were taped with special duct tape to

prevent air leakage. One inch thick fiberglass insulation was wrapped around the entire duct to reduce heat gain from the sur-roundings.

B. The Test Coil

Two finned tube water cooling coils with continuous fins were furnished by Brod and McClung Pace Company of Portland, Oregon. The first coil had four fins per inch and was four rows deep with 12 inch vertical header and 18 inch wide cooling coil. The second coil was the same as the first in all general dimensions except that it had eight fins per inch.

Since the blower used in the air system was equipped with a comparative low power motor, it was decided that the coil with four fins per inch should be selected as the test coil in order that there would be sufficient blower capacity during the frost tests. The front view of the test coil is shown in Figure 3.

The test coil was made of 32 copper tubes, 5/8 inch in dia-meter with 0.020 inch wall thickness. The tubes were positioned in a four-row staggered arrangement. Each row of the tube was con-nected outside the test coil by U-bends. Two 12 inches high, 2-1/4 inches in diameter headers were provided for the test coil on the same side. There were four 5/8 inch copper tube feeders for each header. The antifreeze entered the upper end of the downstream
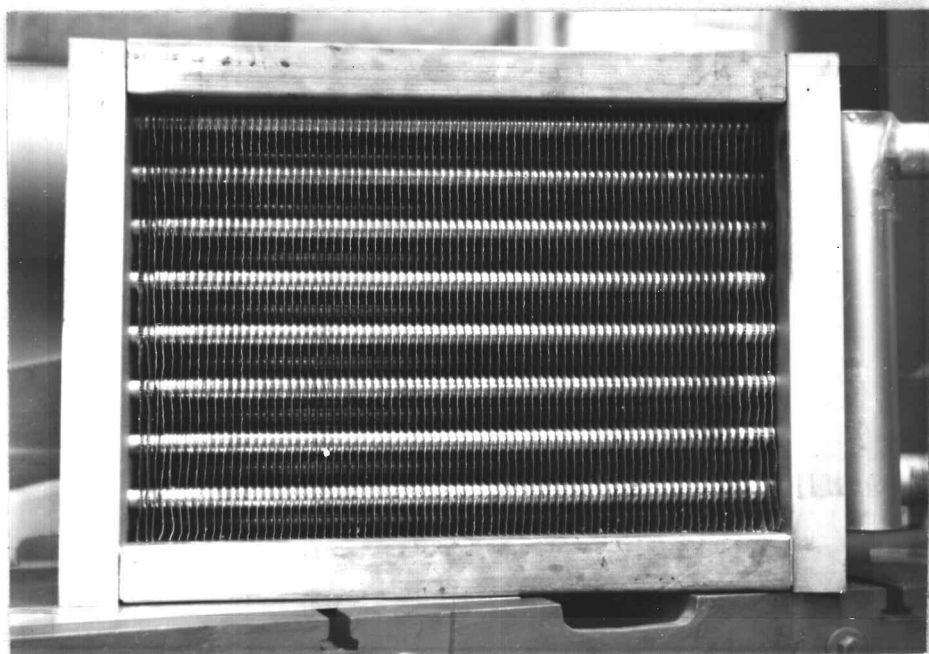
Figure 3.   Front view of test coil.
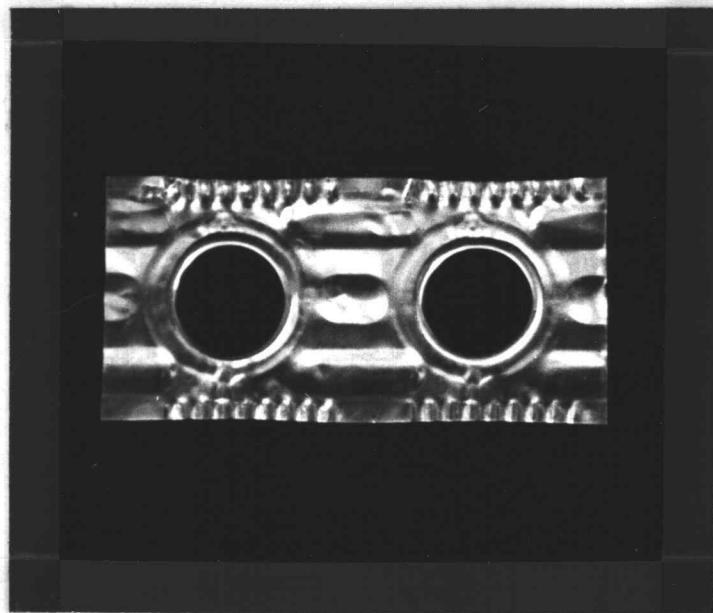
Figure 4.   A close-up of a sample fin.

header and was discharged through the lower end of the upstream header. A small air vent valve was provided at the top of the discharge header. The coil was arranged with counter flow half-serpentine water circuiting in which every other tube in the first row was fed.

The fins were made of continuous aluminum plate 0.0095 inch thick. They were crimped intermittently along the vertical direction and stamped to form small buckets around the tube collars. A photograph of a sample fin is shown in Figure 4.

The net air flow depth of the fins was six inches. The detail of the tube arrangement relative to the fin and the direction of air flow is shown in Figure 5.

There were 77 fins on the test coil. More specifications for the test coil are given in Table 1. For calculation purposes the fins were assumed to be a flat plate of uniform thickness.

The coil with eight fins per inch was used as an auxilliary coil to pre-chill air from room temperature to the desired test conditions.

C. The Antifreeze System

The antifreeze was a 30 percent mixture by weight of ethylene glycol and water. It was chilled to the desired temperature in a circular steel tank equipped with a 1.5 ton Freon-22 refrigeration unit.

15
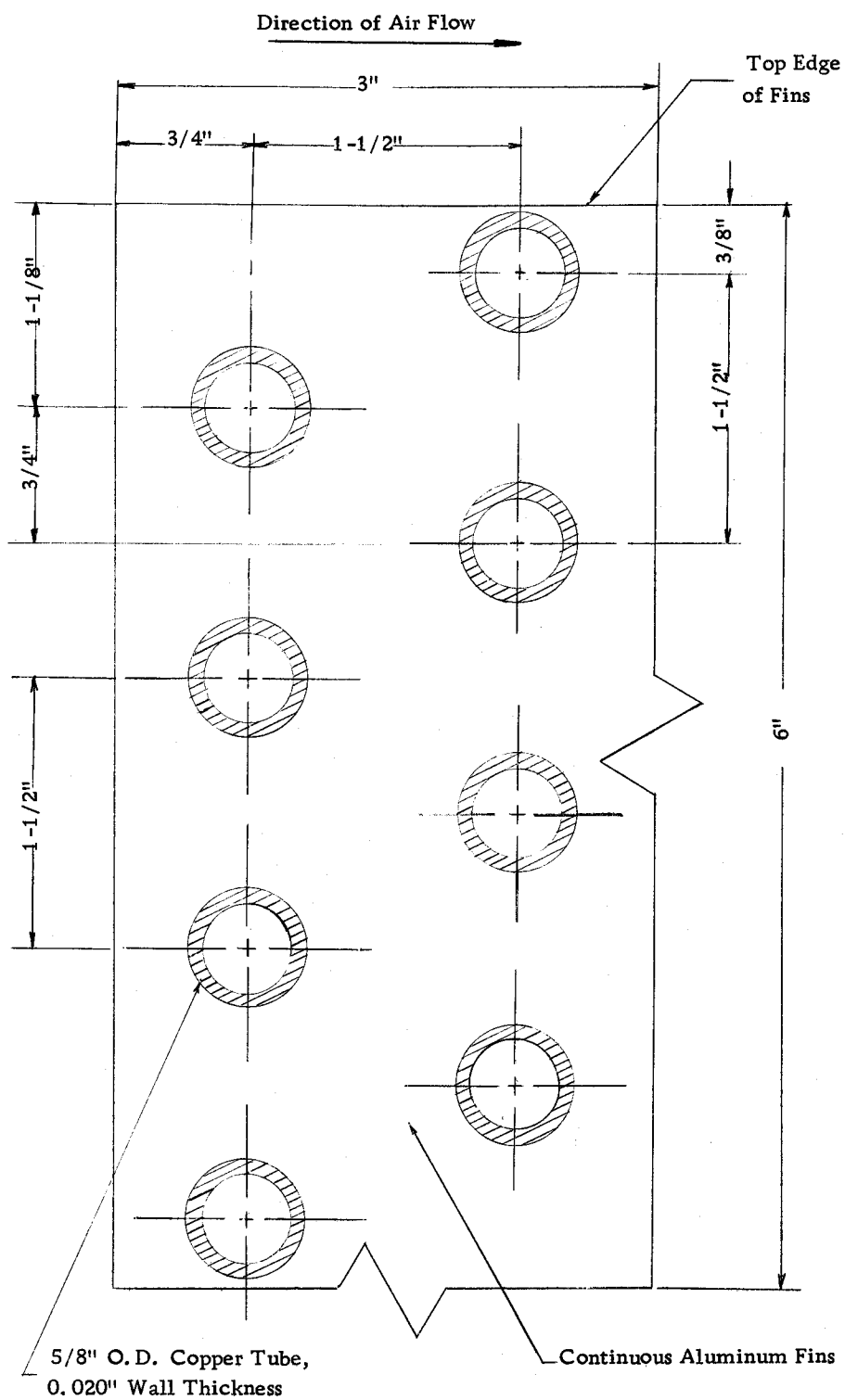
Figure 5. Details of fin and tube arrangement.

Table 1. Test coil surface geometry.

Face Dimensions, inches high by inches wide	12x18
Face Area (A_{fr}), square feet	1.5
Number of Tubes	32
Tube Arrangement	Staggered
Refrigerant-side Area (Ar), square feet	7.35
Fins Area (A_f), square feet	66.60
Total Airside Heat Transfer Area (A_a), square feet	74.45
Fin Area per Total Airside Area (A_f/A_a)	0.895
Total Airside Area per Total Refrigerant-side Area (A_a/A_r)	10.13
Total Airside Area per Total Coil Volume, ft^2/ft^3	99.27
Minimum Free Area (A_{min}), square feet	1.022
Minimum Free Area per Face Area (A_{min}/A)	0.542

A thermostatic type motor control device was used to control the antifreeze temperature by means of a temperature sensing bulb immersed in the chilling tank. The finest setting for compressor motor cut-in and cut-off was about ±2° F.

The antifreeze was drawn through the lower outlet of the chilling tank and distributed to the test coil and auxilliary coil by a centrifugal pump driven by a 1/12 horsepower motor. The antifreeze was returned to the chiller through the top of the tank.

One inch standard pipe was used for the antifreeze piping.
The flow diagram of the antifreeze system is shown in Figure 6. The
rate of flow of antifreeze supplied to the coils was regulated by globe
valves installed in the corresponding supply lines.

An 1/2 inch diameter orifice was installed in the test coil
supply pipe to measure the antifreeze flow rate. The orifice was
provided with vena contracta traps and connected to a U-tube mer-
cury manometer. This orifice was calibrated for weight rate of flow
and the calibration curve is given in Figure 18 in the Appendix.

The entire antifreeze piping was insulated with one inch insu-
lation.

D. The Test Station

The test station included the equipment and instrumentation to
provide the means of measuring the weight of frost on the coil, the
air temperatures and pressure drop across the test coil and the
temperatures of the antifreeze.

The direct measurement of the weight of frost buildup on the
test coil during the test run was accomplished by mounting the test
coil on a platform scale and connecting the test coil to the air system
by flexible connections.

Flexible duct connections were used to connect the test coil to
the air system. They were made of plastic ducting sheet stretched
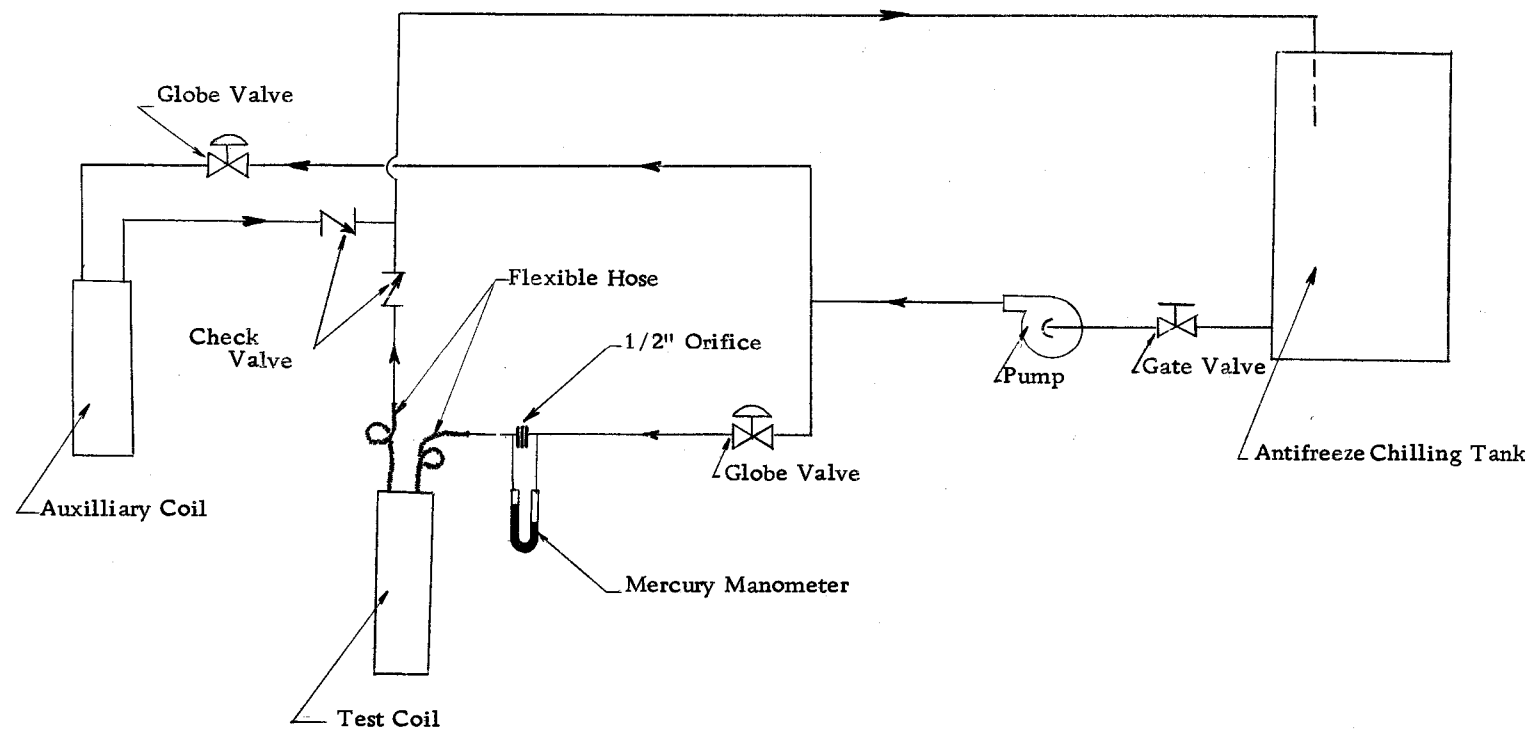
Figure 6. Antifreeze flow diagram.

between two 12 inch by 18 inch short duct frames.

Two pieces of 5-1/2 inch long duct bolted to the test coil flanges acted as the transition sections between the test coil and the flexible duct connections. The method for which the coil was connected to the air system is shown in Figures 7 and 8.

Two flexible hoses were used to connect the antifreeze piping and the test coil headers. Each flexible hose was made of 3/4 inch plain rubber hose, 20 inches long. One of its ends was connected to the antifreeze piping and the other end was bend to form a complete circular loop before it was connected to the coil header.

The scale was manufactured by the Fairbank Morse Company, having 120 pounds total capacity with one ounce graduations. Readings could be estimated to 1/4 ounce. Two hairlines on either side of the beam was made to guard against parallax and allow more accurate reading of the beam. The top of the scale platform was covered by one inch thick fiberglass insulation sheet. The entire test apparatus except the scale were insulated with one inch thick fiberglass insulation. Care was exercised to wrap the insulation loosely at the flexible connections.

Standard weights were placed on the test coil and the readings of scale were taken to check the sensitivity of the weighing system. It was found that for the net weights from zero to four pounds there was negligible effect due to the stiffness of the flexible connections.

Figure 7. The test station.
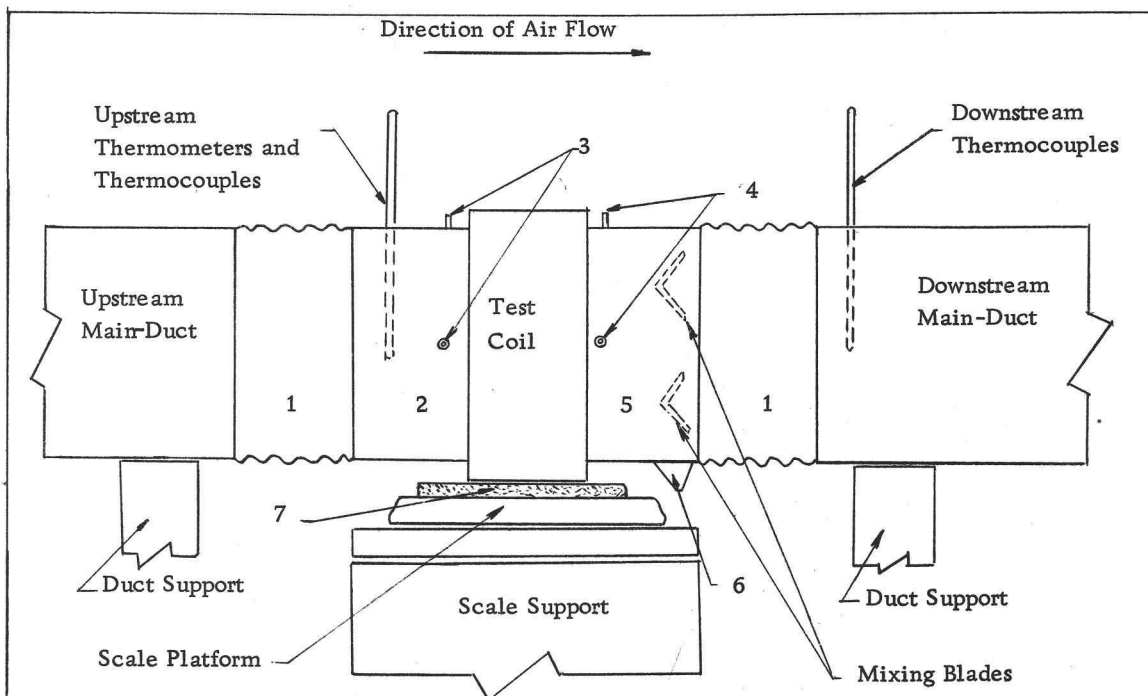
LEGEND

1 Flexible Duct Connections
2 Upstream Transition Duct
3 Upstream Static Pressure Taps
4 Downstream Static Pressure Taps

5 Downstream Transition Duct
6 Condensate Drain Pan
7 Fiberglass Insulation
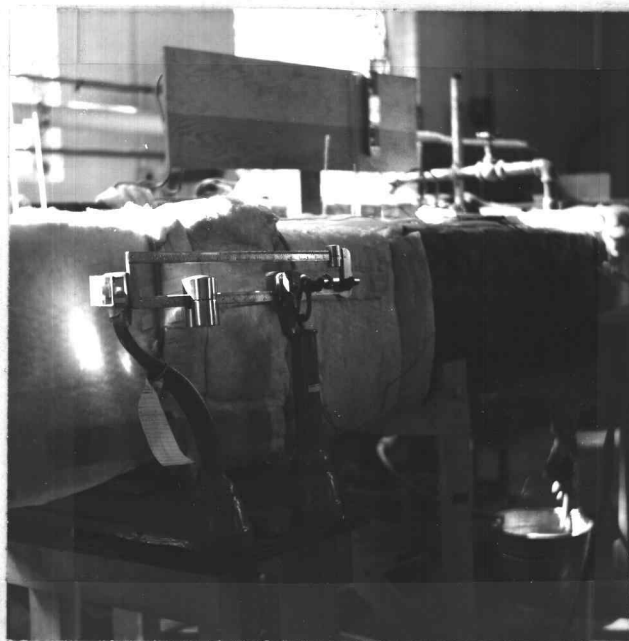
Figure 8. A close-up of the test station.

However, when the net weight exceeded four pounds the stiffness of

the flexible connections caused a significant error between the true

weight and the scale reading. A typical plot between the true weights

and the scale readings is shown in Figure 19 in the Appendix. For-

tunately, the weight of frost accumulated on the test coil throughout

this investigation fell into the range where the stiffness of the flex-

ible connections was negligible.

The conditions of air entering the test coil were measured by

mercury thermometers and thermocouples, located at 3-1/2 inches

ahead of the test coil. A mercury thermometer fitted in a rubber

plug was inserted into the transition duct through the opening provided

at three inches from the top wall center. This thermometer was

used as a direct indication for the entering air dry bulb temperature

so that the temperature could be controlled. A No. 28 gauge copper-

constantan thermocouple was attached to this thermometer along the

glass stem. The thermocouple junction was located at the midpoint

between the top and the bottom duct walls. The reading of this

thermocouple corresponded to the entering air dry bulb temperature

and was used for heat transfer calculations.

Another mercury thermometer was inserted into the transi-

tion duct section by the same method and at the same distance from·

the test coil. It was located three inches from the top wall center,

opposite the first thermometer. This thermometer was also

accompanied by a No. 28 gauge copper-constantan thermocouple

attached to the glass stem. The junction of the thermocouple was

located immediately below the mercury bulb. Both the mercury bulb

and the thermocouple junction were then covered by a thin cotton

fabric which was moistened with water and held in the freezing air

stream to serve as an ice bulb for the thermometer and the thermo-

couple.

The ice bulb thermometer was intended to give direct reading

of the entering air ice bulb temperature for control purposes, while

the reading through the ice bulb thermocouple gave the true air ice

bulb temperature.

The temperature of air leaving the test coil was measured by

a set of four copper-constantan thermocouples located 18 inches

downstream. Each thermocouple was fastened to a glass rod which

was inserted into the hole provided on the top wall of the main duct

by a rubber plug. All thermocouple junctions were located halfway

between the top and bottom duct walls. The four thermocouples were

connected in parallel to allow direct reading of the average air tem-

perature leaving the test coil.

In order to ensure that the air leaving the test coil was well

mixed at the thermocouples station, two V-shaped mixing blades

were placed horizontally across the transition duct four inches from

the downstream side of the test coil. The mixing blades were so

positioned that the V-notch pointed against the air stream.

The antifreeze temperatures entering and leaving the test coil were measured by thermocouple probes inserted vertically into the headers of the test coil. Each thermocouple probe was made of 1/4 inch copper tubing about nine inches long soldered one end to a bushing. Four No. 28 gauge copper-constantan thermocouples were inserted into the probe tubing. The thermocouple junctions were brought out from the inside through the holes provided in such a way that when the probe was inserted into the header each thermocouple junction would be located close to a feeder tubing connecting the coil and the header. All the holes from which the thermocouple junctions were brought out were filled with epoxy resin to prevent the leakage of antifreeze into the thermocouple probe tube. Approximately 3/4 inch of bare wires were exposed to antifreeze at each thermocouple junction in order to minimize the effect of the heat conduction along the wires. Care was taken to prevent the wires from touching each other or being shorted at the copper tube wall. The probe for inlet header was inserted into the header through the top wall while the probe for outlet header was inserted through the bottom wall.

The four thermocouples at each probe were connected in parallel in order that the temperature readings would represent the average antifreeze temperature.

All the thermocouple leads were connected to a selector-switch. The cold junction was made from a copper-constantan thermocouple immersed in a thermos bottle filled with a mixture of crushed ice and water. It was connected in series with the selector-switch and a potentiometer.

The Leads and Northrup precision potentiometer No. 8686 had a range between -10.1 to +100.1 millivolts with 0.005 millivolt smallest divisions was used for thermocouple readings throughout this experiment.

Static pressure taps were provided at 1-1/2 inches pre-ceeding and following the test coil. At each location there were three static pressure taps each located at the center of the transition duct walls at the top and both sides. The three static pressure taps at each location were connected to a common rubber tubing leading to the positive or negative pressure chamber of a vertical water micro-manometer from which the pressure drop across the test coil was measured. The water micro-manometer was the same type as the one used for measuring the air pressure drop across the orifice in the air system.

A condensate pan was provided at the bottom of the down-stream duct transition section to drain the melted frost from the coil after the test run was completed.

CHAPTER III

EXPERIMENTAL PROGRAM AND PROCEDURE

Experimental Program

The experiments were carried out with three air flow rates
585, 685 and 775 CFM respectively with the entering air condition
maintained at approximately 32 degrees Fahrenheit and specific
humidity of 0.003 pound of water vapor per pound of dry air. The
antifreeze supplied to the test coil was kept constant at approxi-
mately 14 degrees Fahrenheit and the flow rate of 1853 pounds per
hour.

Sufficient data were recorded to determine the overall heat
transfer coefficient, and the air pressure drop associated with various
degrees of frost buildup on the test coil.

Experimental Procedure

A. Preliminary Preparations

The following step-wise preliminary preparations were
necessary prior to each test run.

1. The room temperature and the barometric pressure were

recorded.

2. The potentiometer was adjusted for mechanical zero and standardized. The cold junction of the thermocouple was immersed in a thermos bottle filled with the mixture of crushed ice and water.

3. Both of the water micro-manometers used for measuring air pressure drop across the test coil and the orifice were leveled and zeroed.

4. The humidifier pipe including its piping was completely drained.

5. The scale for weighing the frost weight was checked for sensitivity by standard weight. The level of the adjacent duct supports and the hair lines for beam were adjusted if necessary to give the best scale sensitivity. The scale tare weight was recorded.

6. The refrigeration unit for the antifreeze chiller was started and the thermostatic temperature control was set to 14 ± 2 degrees Fahrenheit. The antifreeze pump was started and the antifreeze was circulated through the auxilliary coil.

7. The blower was started after the antifreeze had been chilled to the desired temperature. The air in the system was then chilled through the auxilliary coil to about 25 degrees Fahrenheit and maintained at this temperature until the next step was completed.

8. The cotton fabric covering the ice bulb thermometer and thermocouple was moisted with water and inserted into the duct. Care

was taken to check that it was completely frozen.

B. Test Procedure

1. The dry bulb temperature of the air in the system was gradually

increased to 32 degrees Fahrenheit through the control of

electric heater's supply voltage and the flow rate of the anti-

freeze in the auxilliary cooling coil. The ice-bulb temperature

was maintained at approximately 30 degrees Fahrenheit by

varying the steam supply rate to the humidifier. After the en-

tering air condition was established it was maintained constant

for about 15 minutes in order to make sure that there would be no

abrupt changes.

2. The air flow rate was then adjusted to the desired value by the

regulation of damper and the reading of the pressure drop

across the airflow orifice.

3. The antifreeze was allowed to flow through the test coil at con-

trolled rate indicated by the mercury manometer pressure dif-

ferential at the orifice. The air vent valve on the discharge

header was opened to purge air from the header. The air that

might be collected in the manometer lines was also purged.

4. The scale was immediately rechecked for sensitivity and change

in tare weight.

5. The temperatures of air and antifreeze, the pressure drop across

the test coil were recorded at each significant frost buildup during the test run. The entering air condition, air flow rate, the antifreeze temperature of the supplying antifreeze and its flow rate were maintained as constant as possible.

It was observed through many trial runs that during the frost test the condition of air and antifreeze would vary very little in a short time interval. It was, therefore, possible to assume that quasi-steady state was reached as the readings were taken. Usually several trial runs were necessary for each series of tests in order to gain sufficient experience in the control and manipulation of the system.

The duration of test run was dictated by the blower capacity. The tests were run until the pressure drop in the system was so great that the blower could no longer deliver the desired air flow rate. After each run the antifreeze flow to the test coil was terminated and the frost was melted by circulation of heated warm air. The condensate was completely drained through the drain pan. Circulation of warm air was continued for several hours to insure that the test coil surface was clear from condensate.

CHAPTER IV

RESULTS AND DISCUSSIONS

A. Heat Transfer Results and Discussion

1. Heat transfer results

The overall heat transfer coefficients, U, were plotted against the frost intensities, X, in Figures 9, 10 and 11, corresponding to the air flow rate of 585, 685 and 775 cubic feet per minute respectively. These curves are again shown in Figure 12 for comparison.

The overall coefficient of heat transfer is calculated by equation (4) and having the units of Btu per hour per square foot -°F. The frost intensity, X, is expressed in grains of frost per square foot of airside heat transfer area. The air flow rates were based on the standard air of 0.075 pound per cubic foot density.

All the curves were obtained by fitting the data points with a least square polynomial by a digital computor. The least square equations for various air flow rates are presented in Table 2.

The computed values for the overall heat transfer coefficients are tabulated in Tables 4, 5 and 6 in the Appendix.
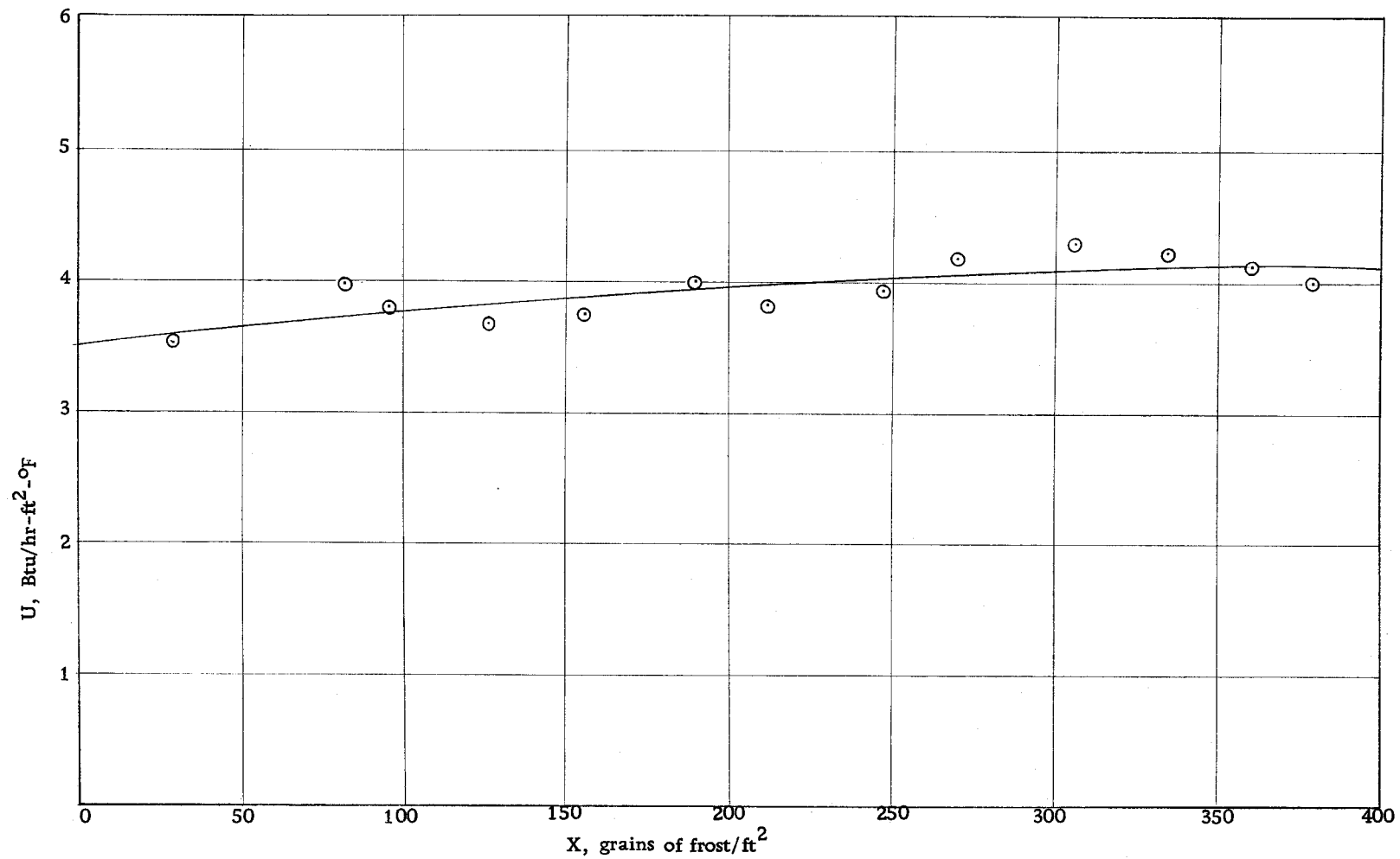
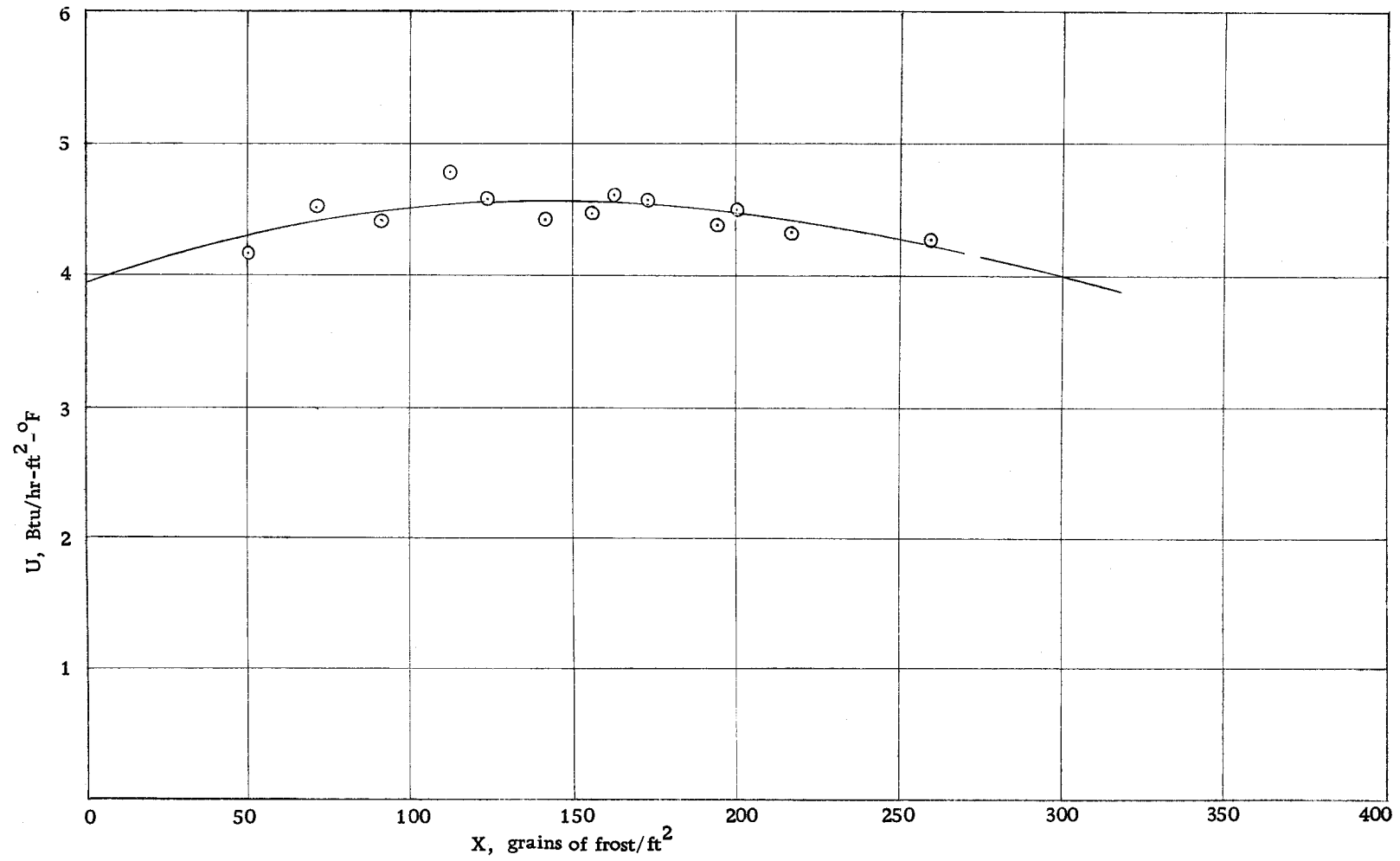Figure 9.   Variation of U at 585 CFM.

Figure 10. Variation of U at 685 CFM.
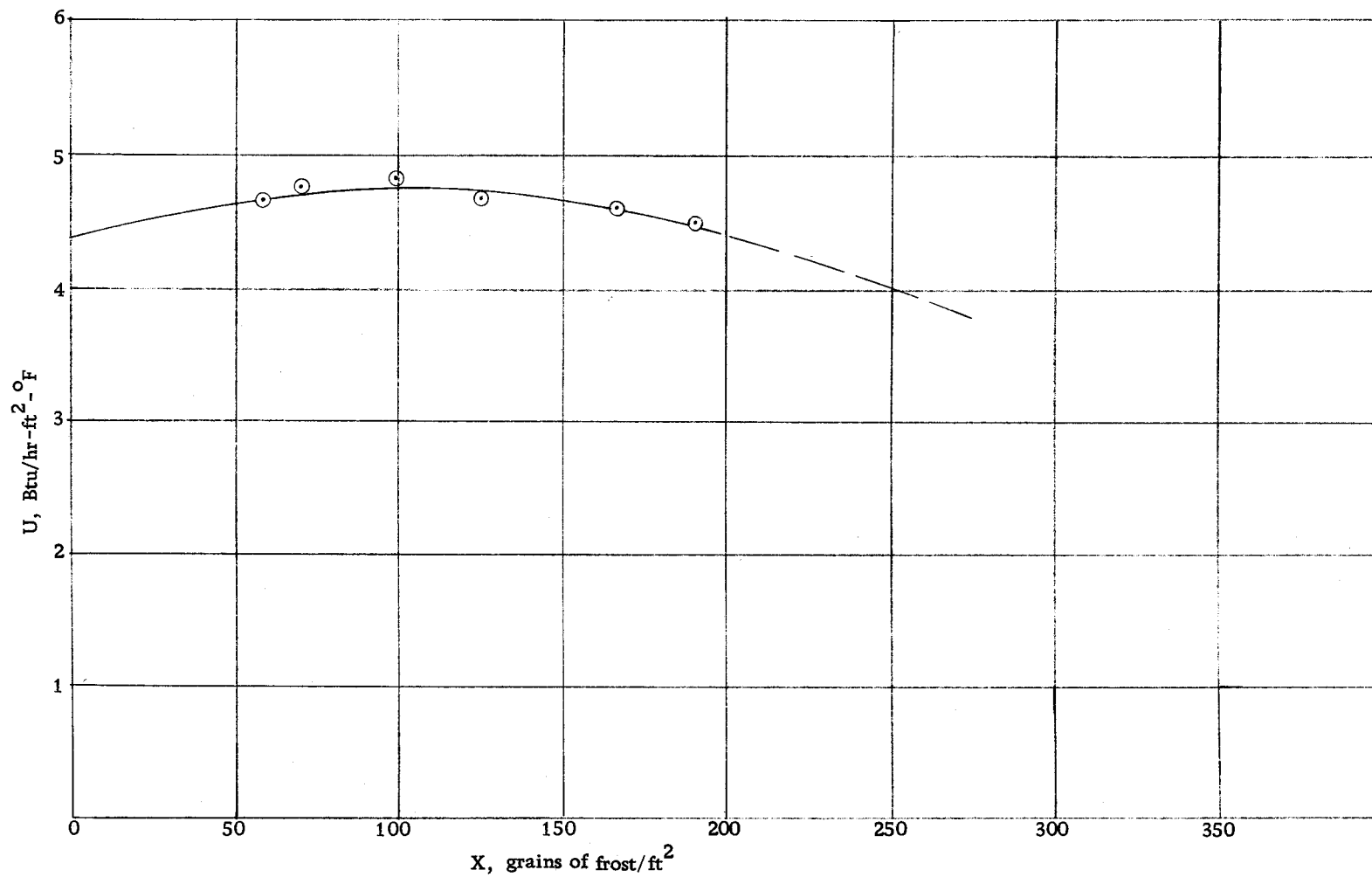
Figure 11. Variation of U at 775 CFM.
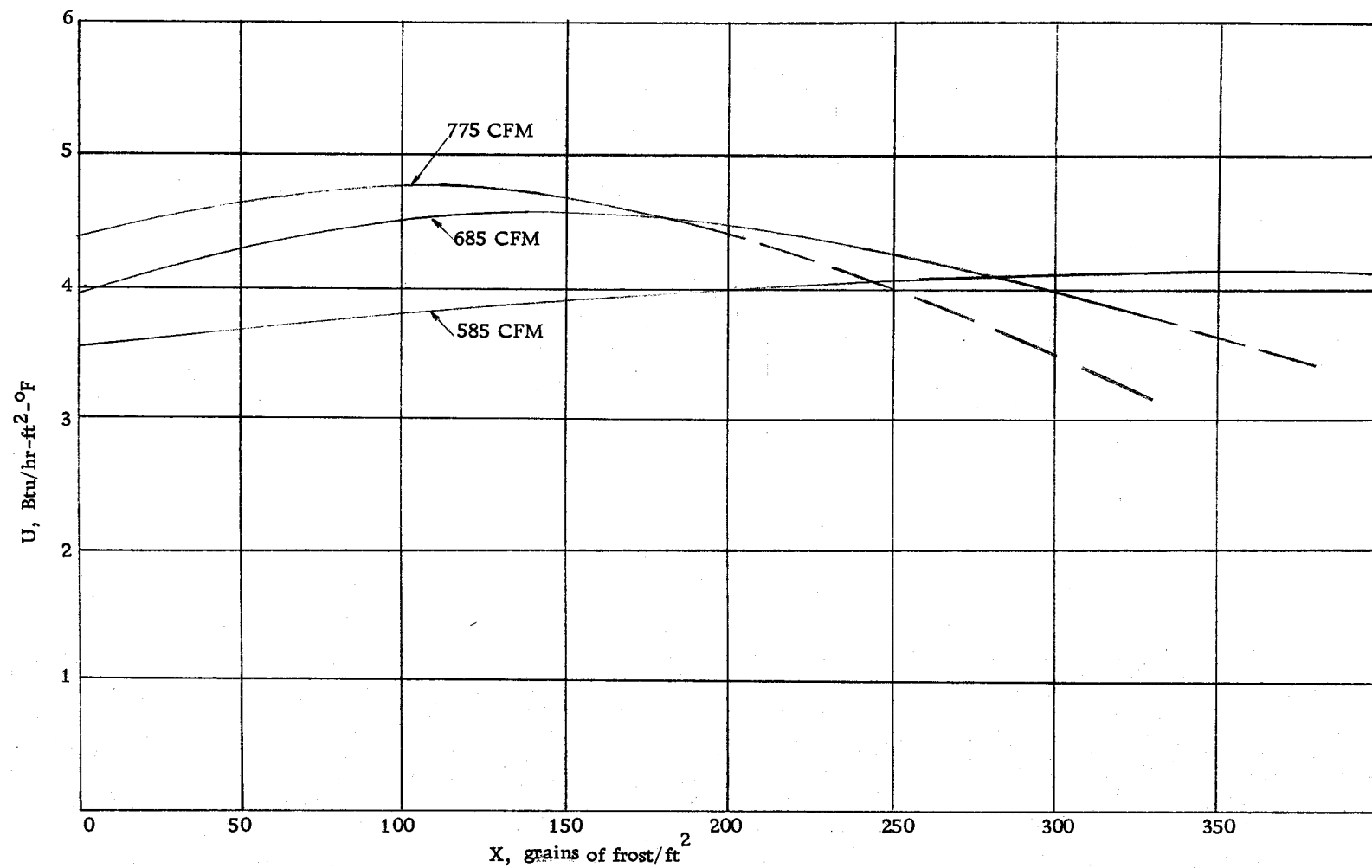
Figure 12. Effect of air flow rate on U.

Table 2. The least square equations for the heat transfer data.

Air Flow Rate	Least Square Equations
585 CFM	$U = 3.5279 + 0.26999 \times 10^{-2}X - 0.27822 \times 10^{-5}X^2$
685 CFM	$U = 3.9653 + 0.82158 \times 10^{-2}X - 0.28301 \times 10^{-4}X^2$
775 CFM	$U = 4.3556 + 0.76879 \times 10^{-2}X - 0.37532 \times 10^{-4}X^2$

2. Discussion

In each of the Figures 9, 10 and 11 it appears that the U

values first increased with increasing frost intensity on the coil sur-

face. When the increase in the U value reached a peak, further in-

crease in frost intensity on the coil had the effect of decreasing the

U values. This trend seems to agree with the observation made by

Stoecker[6], although his work was based on finned coils of different

type of fins and coil geometry.

The increase of the overall heat transfer coefficients during

the light deposit of frost on the coil surface could probably be due to

two major reasons: the increase of airside film coefficient of heat

transfer and the increase in effective heat transfer surfaces.

The increase of airside film coefficient of heat transfer is

explained by the fact that air film coefficient of heat transfer in-

creases with increasing air velocity which affects the degree of air

turbulence. The layer of frost on the coil surface causes not only an increase in the amount of turbulence due to the roughness of frost but also an increase in air velocity because of reduced flow area through the coil. The increase of effective heat transfer sur- face was essentially due to the extension of the coil surface area by the frost layer.

The decrease in the overall heat transfer coefficients after the peak is reached could be due to the insulation effect of frost on the heat transfer surface. This insulation effect was caused by the thickening of frost layer on the coil surface. Apparently, the in- crease in air film coefficient of heat transfer and the increase in effective heat transfer surfaces, at this instant, were not sufficient to compensate the increase in the thermal resistance of the frost. It was also expected that the increase in airside heat transfer co- efficient at this region was relatively low when compared to the in- crease during the lighter frost intensity. This is because the high thermal resistance of the thickened frost reduced the temperature gradient at the frost-air interface.

Closer examination of Figure 12 reveals that at higher flow rate U assumes higher values and that the peak is reached at lower frost intensity than the one at the lower flow rate because of the above mentioned reasons. But at higher air flow rates the decrease in U after the peak value with increasing frost intensity is more abrupt.

This behavior can possibly be explained, among other reasons, by the possible interference of the boundary layer on rough frosted surface between the adjacent fins, which is caused by high air flow rate having forced through the narrowed air passages. At the lower air flow rate, however, the value of U after the peak value decreases more gradually with increasing frost intensity as the rate may not be sufficiently high to cause interference effect of boundary layer. The observation that U values are higher for higher air flow rates conformed to the principle of heat transfer.

The reduction of the U values at heavier frost intensity has certain effect to a refrigeration system. When a coil is selected based on a design condition and capacity, the air flow rate, the entering and leaving air conditions are automatically fixed. Therefore, the reduction in the U values must be compensated by an increase in the mean temperature difference between the refrigerant and the air. This can be seen from equation (2) which is used to define U as follows:

$$U = \frac{60 \ \overset{\circ}{m}_a \ c_p \ (t_{a_1} - t_{a_2})}{A_a \ \Delta T_m}$$

where $60 \ \overset{\circ}{m}_a \ c_p \ (t_{a_1} - t_{a_2})$ is fixed for a fixed refrigeration capacity and design condition. The coil area, A_a, is also fixed by the coil selected. The increase in the mean temperature difference between the refrigerant, ΔT_m, calls for a lower refrigerant temperature,

since

$$\Delta T_m = \frac{t_{a1} - t_{a2}}{\ln \dfrac{t_{a1} - t_r}{t_{a2} - t_r}}$$

where t_r and ΔT_m are the variables. It is evident that the reduction

of the refrigerant temperature will have an effect to the system econ-

omy. Since the lower the refrigerant temperature, the lower is the

coefficient of performance.

Therefore, the amount of the decrease in system efficiency

could be predicted based on the knowledge of the behavior of U

values for the coil operating under frosting conditions.

B. Pressure Drop Results and Discussion

1. Pressure drop results.

The pressure drops, ΔP, were plotted against the frost in-

tensities, X, in Figures 13, 14 and 15 with air flow rates of 585, 685

and 775 cubic feet per minute respectively. Figure 16 shows the

comparison of pressure drop curves at various air flow rates.

All the pressure drop data were converted to inches of water

at 70 degrees Fahrenheit. The least square polynomials representing

these pressure drop curves are listed in Table 2. The data for pres-

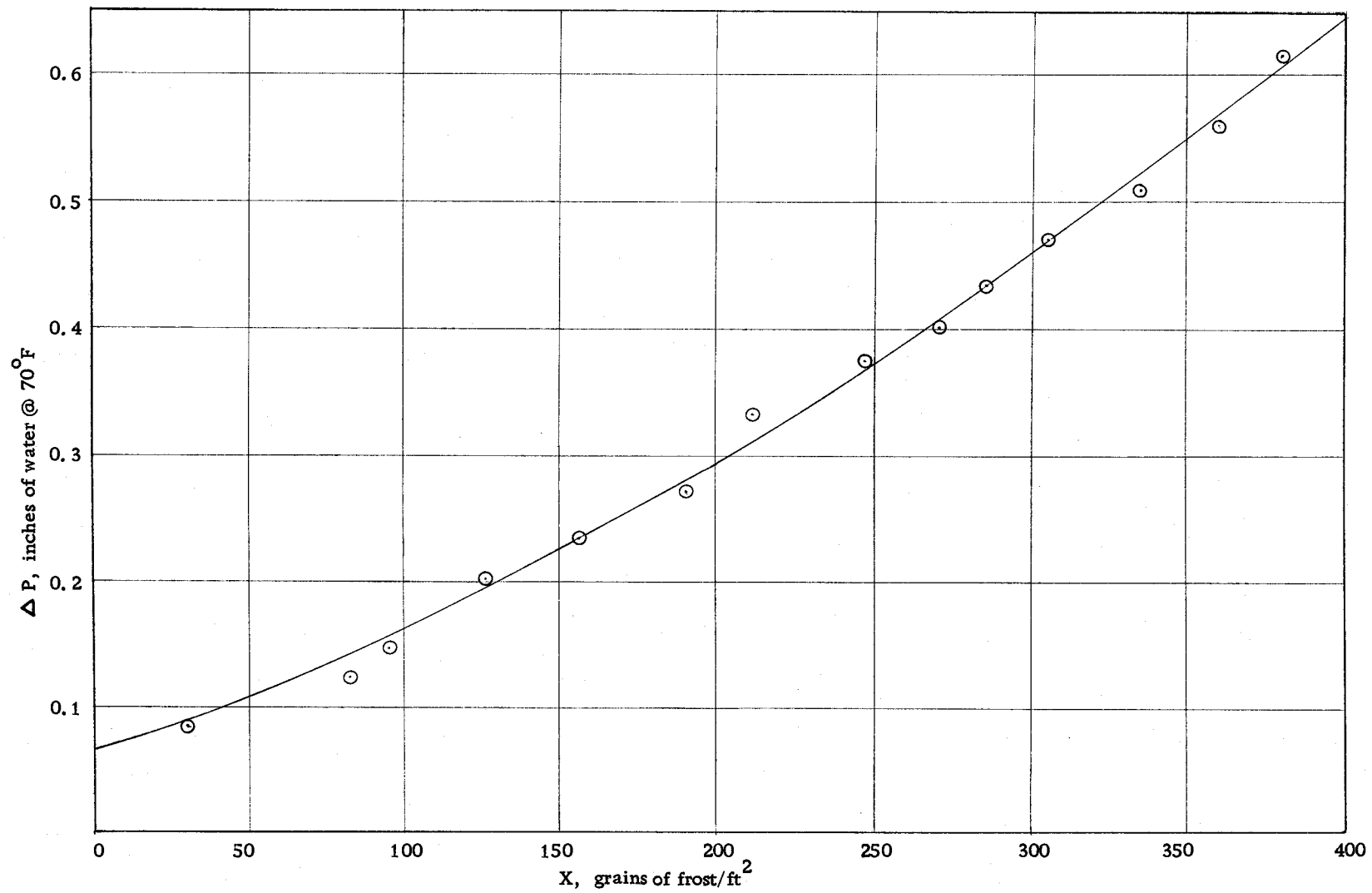sure drop were included in Tables 4, 5 and 6 in the Appendix.

Figure 13. Variation in ΔP at 585 CFM.
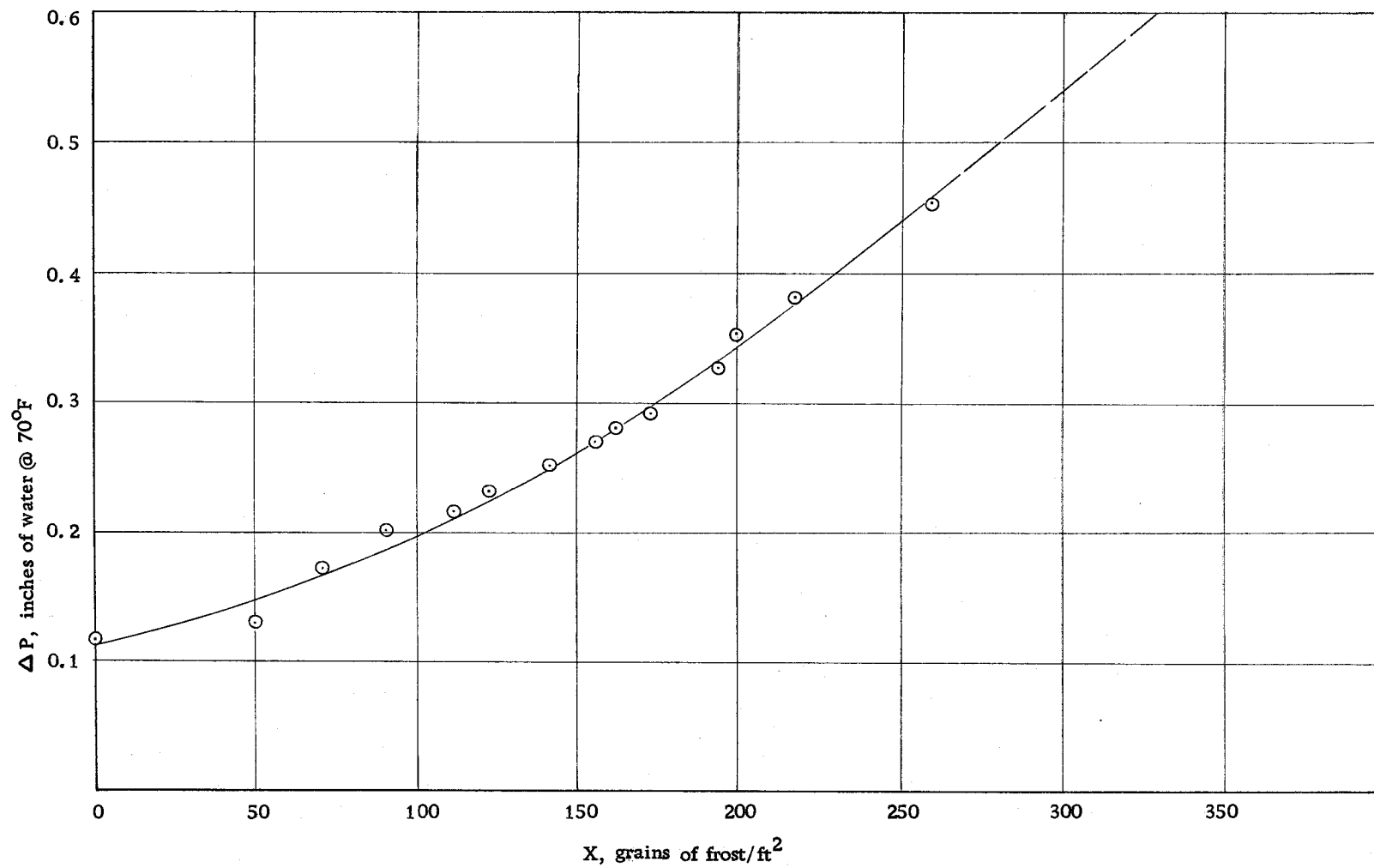
Figure 14. Variation in ΔP at 685 CFM.
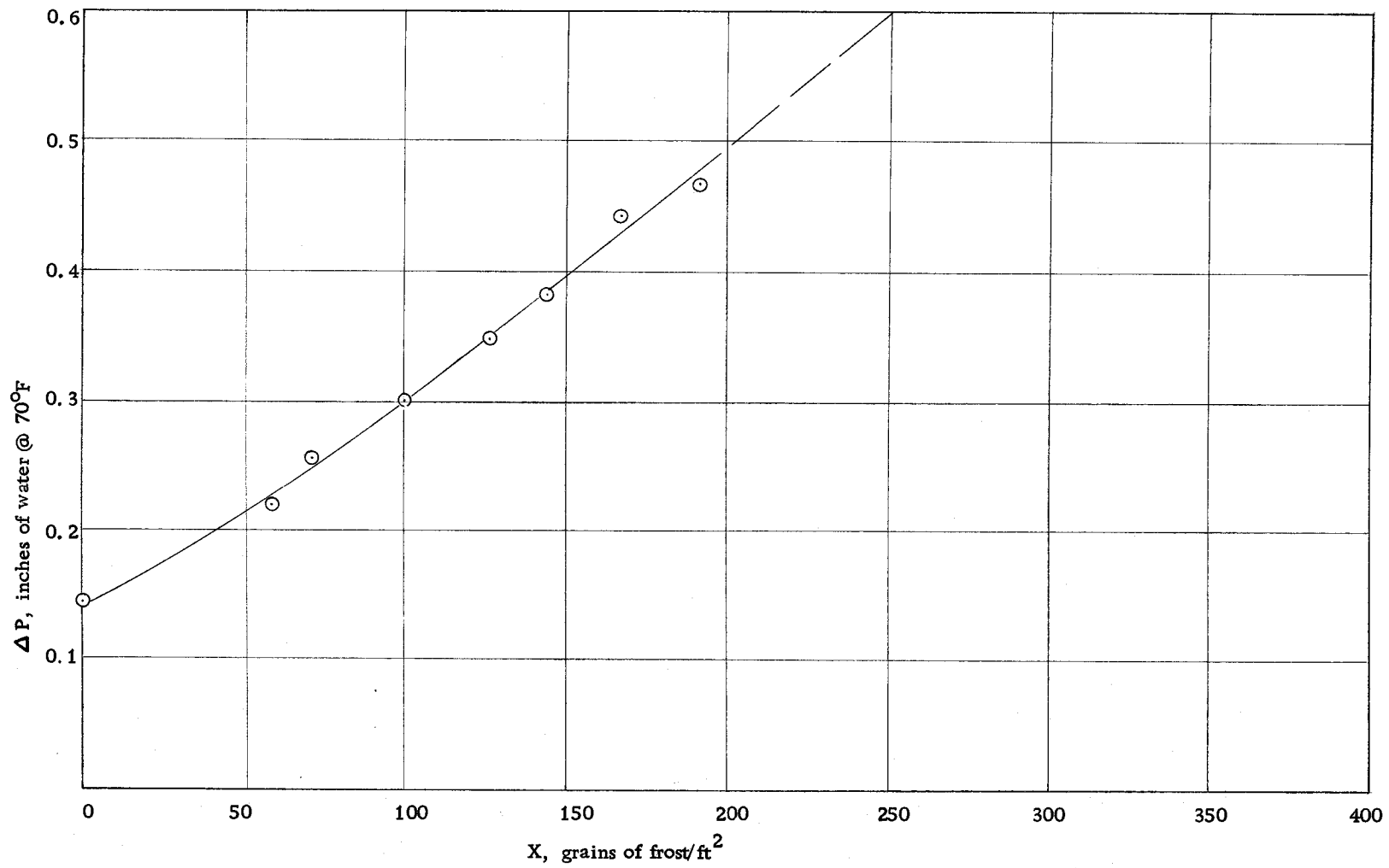
Figure 15. Variation in ΔP at 775 CFM.
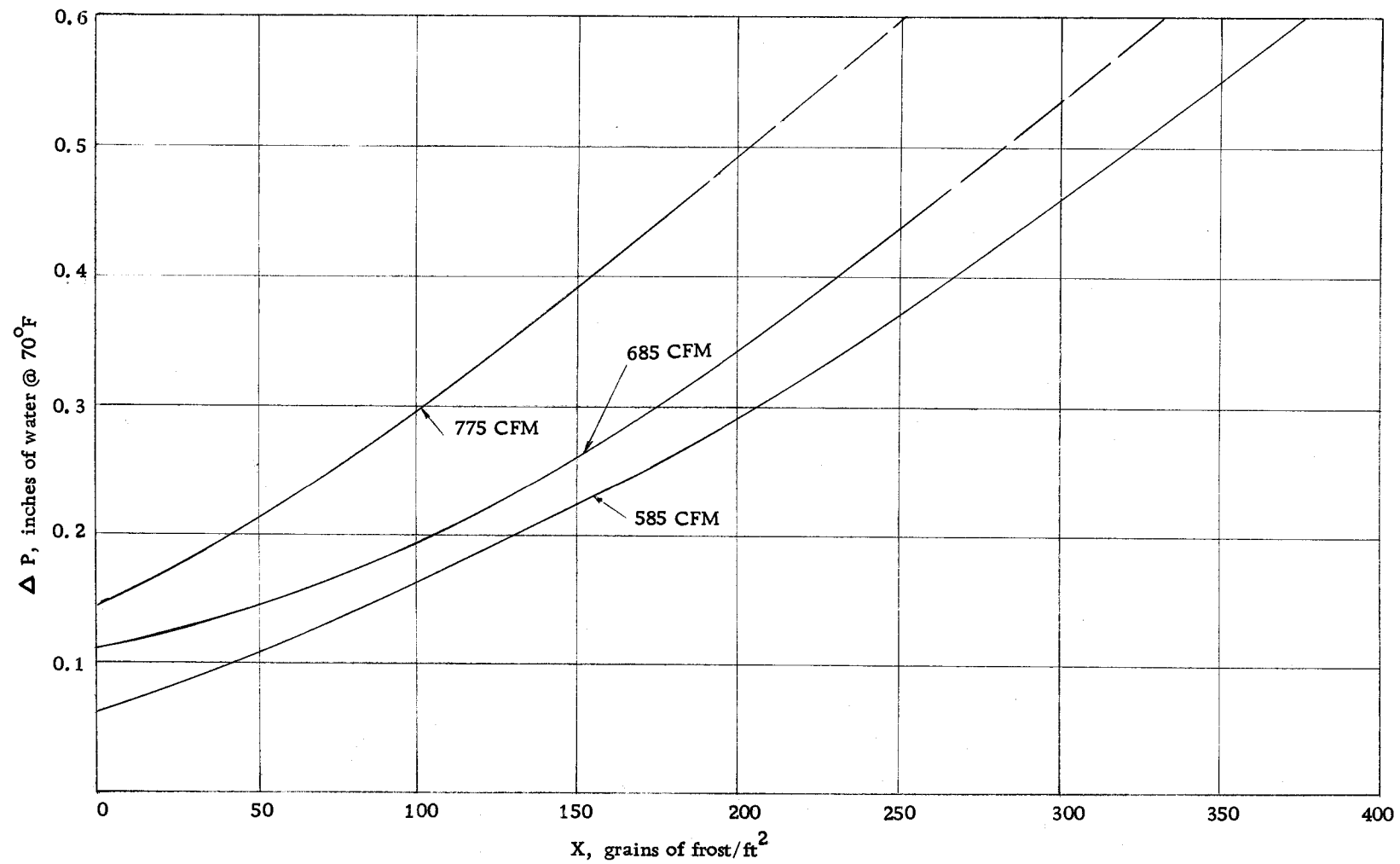
Figure 16.   Effect of air flow rate on ΔP.

Table 3. The least square equations for pressure drop data.

Air Flow Rate	Least Square Equations
585 CFM	$\Delta P = 0.61866 \times 10^{-1} + 0.85179 \times 10^{-3}X + 0.15582 \times 10^{-5}X^2$
685 CFM	$\Delta P = 0.11226 + 0.59021 \times 10^{-3}X + 0.28481 \times 10^{-5}X^2$
775 CFM	$\Delta P = 0.14126 + 0.13884 \times 10^{-2}X + 0.19551 \times 10^{-5}X^2$

2. Discussion

It is evident from Figure 16 that the pressure drop of the coil at the lower air flow rate was quite gradual as the frost intensity increased when compared to the pressure drop at higher air flow rates.

This trend agrees with the principle of fluid flow where the pressure drop increases with increasing air velocity. At low air flow rate the increase in air velocity due to narrowing of air passage caused by frost thickening on the coil surface was not high and hence produced a comparatively low pressure drop. However, at higher air flow rate the increase in air velocity could be much higher and thus creates greater pressure drop across the coil, because the pressure drop is proportional to the square of the velocity.

Furthermore, the roughness of the frosting surface also contributed a great deal to the increase in pressure drop due to the

increase in the flow friction which becomes quite significant at high air velocity.

The increase in pressure drop during the frost formation on the coil surface could affect a refrigeration system in the sense that the air flow rate would be reduced. This decrease in air flow rate would cause reduction in system capacity since a specific amount of chilled air is required to produce certain refrigeration capacity.

The magnitude of air flow reduction during the frosting operation depends on the blower characteristic and the system characteristic. It is apparent that the reduction in air flow would be quite severe when the frost intensity on the coil is high.

Through the knowledge of the pressure drop behavior of the frosted coil, the blower or fan could be selected to handle pre-determined amount of air for the desired refrigeration capacity with greater confidence.

CHAPTER V

CONCLUSIONS AND RECOMMENDATIONS

It may be concluded that the U value increased at light frost intensity and decreased as the frost intensity became higher. The magnitude of the U value is greater at higher air flow rates. However, the U value started to decrease rather abruptly at the higher air flow rate at a comparatively low frost intensity. The pressure drop across the frosted coil depends on the air flow rates. It was observed that the magnitude of the increase in pressure drop per unit increment in frost intensity is larger at the higher air flow rate than at the lower air flow rate. In the view that the behavior of the U values and the pressure drop in the present investigation agreed with the observation made previously by Stoecker (6), who investigated the frosted finned coils with in-line tubes arrangement, it was apparent that the behavior of the U and the pressure drop for the frosted finned coils was independent of the coil geometry.

To the application of frosted finned coil in a refrigeration system, the behavior of both U and pressure drop suggested that a lower coil face velocity was preferable if the interval between defrosting cycle is to be kept sufficiently long. However, compromising between the effect of frost on U and the pressure drop would

be necessary in order to obtain the best economical design.

The results from the present investigation is far from being complete. It is recommended that more research should be done along this line for various air flow rates, type of coils, fin spacing and operating conditions encountered in applications. The future research should be directed toward the obtaining of data, formulas, charts and calculation procedures for the economical design of refrigeration system operating under frosting conditions.

The present weighing system developed for continuous measurement of the frost weight on the test coil proved to be quite satisfactory. However, it could have been better if a set of calibrated load cells were used instead of the platform scale. This would not only give a more sensitive and accurate weighing system but also permit the continuous recording of weights if desired. Automatic controls for the control of the test conditions would be required if the test conditions should have to be varied in the wide range. The present manual control of test conditions is rather laborious and is not suitable for the project involving many tests at various test conditions.

BIBLIOGRAPHY

1. Beatty, K. O., E. P. Finch and E. M. Schoeborn. Heat transfer from humid air to metal under frosting conditions. Refrigerating Engineering Journal 59:1203-1207. 1951.

2. Chung, P. M. and A. B. Algren. Frost formation and heat transfer on a cylinder surface in humid air cross flow. Transactions of the American Society of Heating, Refrigerating and Air Conditioning Engineers 65:213-228. 1959.

3. Lopper, J. L. Frost formation upon a thin aluminum tank containing liquid oxygen. Transactions of the American Society of Heating, Refrigerating and Air Conditioning Engineers 66: 104-113. 1960.

4. Omelianchuk, Paul P. Evaporator frost performance in an ice cream display case. American Society of Heating, Refrigerating and Air Conditioning Engineers Journal 1:87-90. 1959.

5. Stoecker, W. F. Frost formation on refrigeration coils. Transaction of the American Society of Heating, Refrigerating and Air Conditioning Engineers 66:91-103. 1960.

6. _____. How frost formation on coils affects refrigeration system. Refrigeration Engineering Journal 65: 42-46. February, 1957.

7. Weber, M. E. Heat transfer to a cryogenic surface under frosting conditions. Summary of Ph. D. thesis. Cambridge, Massachusetts Institute of Technology, 1964. 15 numb. leaves.

8. Whithurst, C. A. An investigation of heat and mass transfer by free convection from humid air to metal plate under frosting conditions. Ph. D. thesis. College Station, Texas A and M University, 1962. 243 numb. leaves.
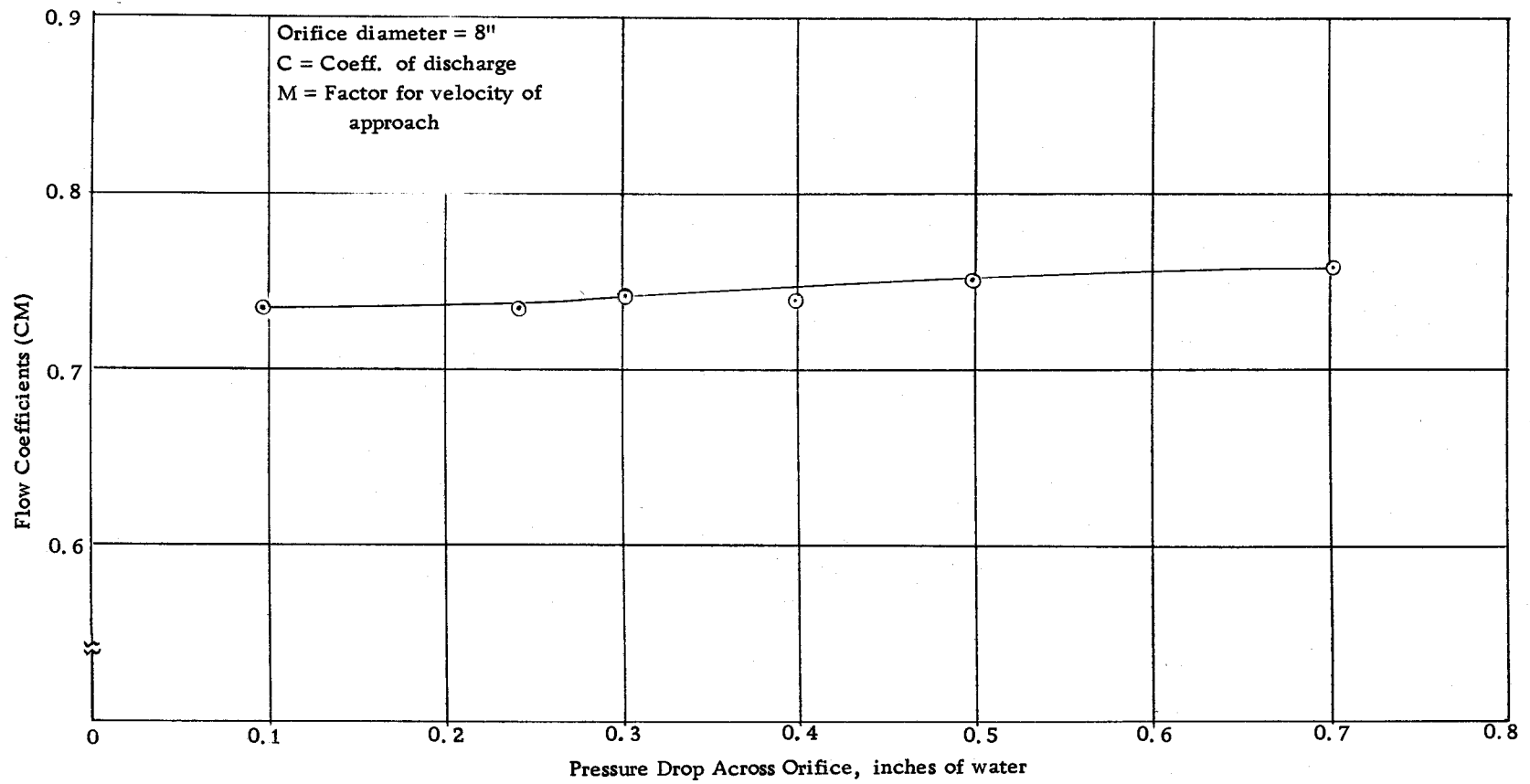
APPENDIX

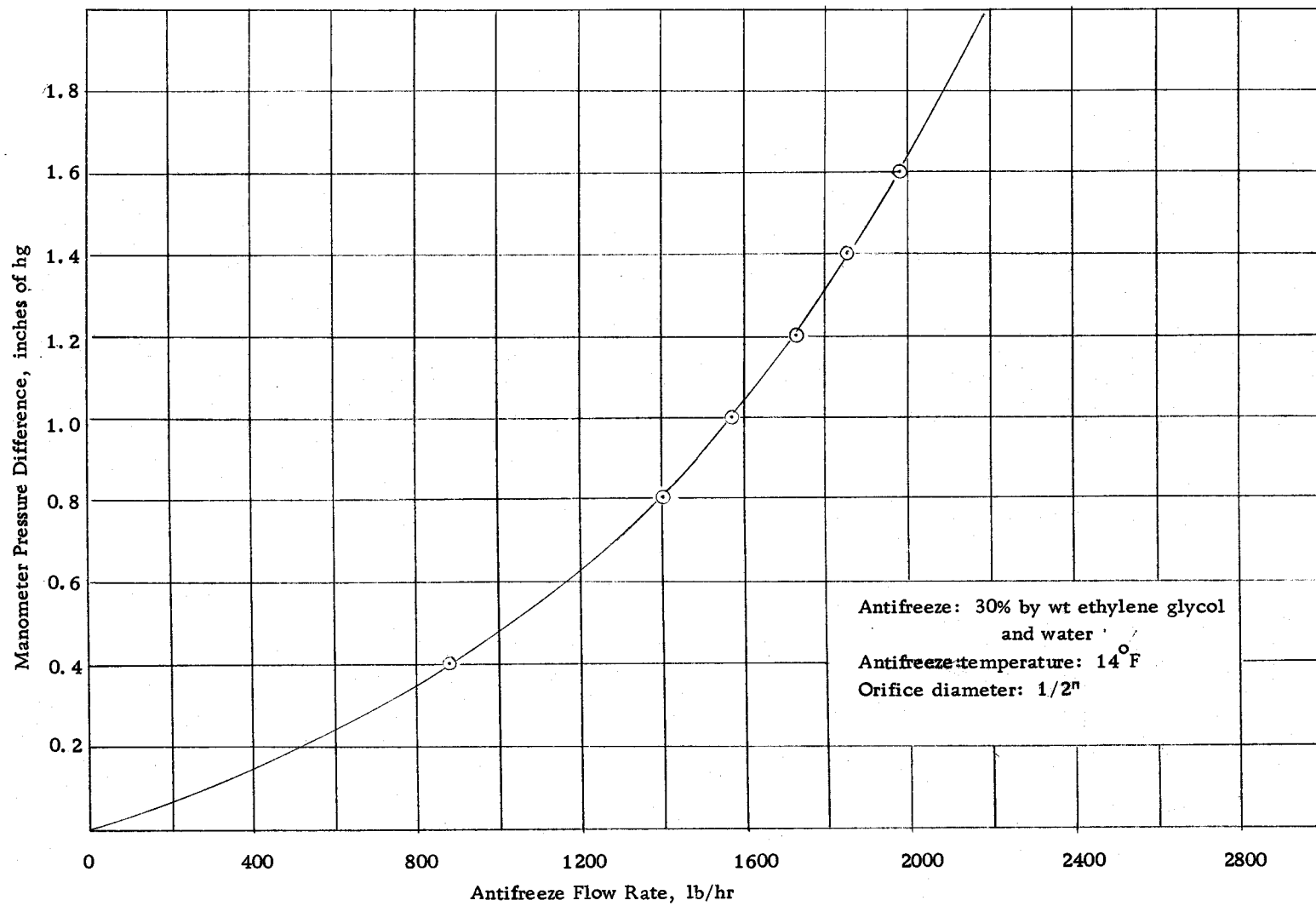Figure 17.   Flow coefficients of air flow orifice.

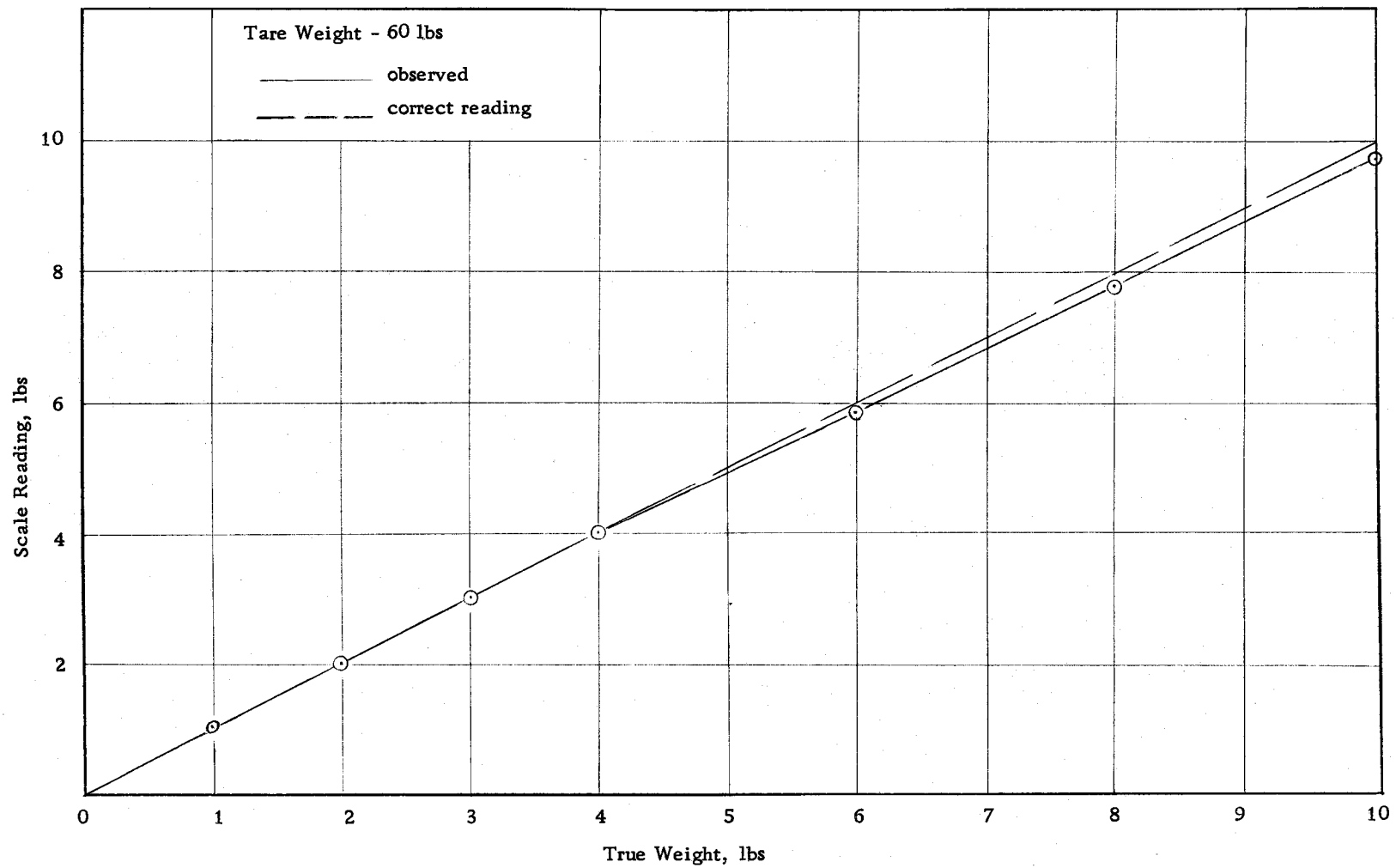Figure 18. Calibration curve for antifreeze orifice.

Figure 19. A typical plot of true weight vs scale reading.

Table 4. Computed data for air flow rate of 585 CFM.

X Grains Frost / ft^2	ΔP in H$_2$O @ 70°	AIRSIDE						ANTIFREEZE			$t_{a_1}-t_{r_m}$ °F	$t_{a_2}-t_{r_m}$ °F	$\ln \dfrac{t_{a_1}-t_{r_m}}{t_{a_2}-t_{r_m}}$	U Btu/hr-ft^2-°F
		t_{a_1} °F	t_{w_1} °F	W_1 lb/lb$_a$	$\overset{\circ}{m}_a$ lb/min	t_{a_2} °F	Δt_a °F	t_{r_1} °F	t_{r_2} °F	t_{r_m} °F				
0	0.07750													
29.3820	0.08310	31.80	30.58	0.0033	43.87	26.16	5.64	13.79	16.86	15.32	16.48	10.84	0.418	3.546
82.2690	0.12340	31.25	29.65	0.00309	43.9	25.12	6.13	13.44	16.38	14.91	16.34	10.21	0.470	3.990
95.4920	0.14740	31.10	29.46	0.00303	43.9	25.22	5.88	13.44	16.18	14.81	16.29	10.41	0.447	3.795
126.3430	0.19980	31.30	29.75	0.00310	43.91	25.41	5.89	13.40	16.13	14.76	16.54	10.65	0.432	3.668
155.725	0.23430	31.34	29.70	0.00307	43.91	25.41	5.93	13.25	16.10	14.68	16.66	10.73	0.440	3.736
189.515	0.27170	31.25	29.52	0.00302	43.91	24.99	6.26	13.20	15.95	14.58	16.67	10.41	0.471	4.000
211.550	0.33260	31.39	29.80	0.00306	43.88	25.41	5.98	13.20	15.95	14.58	16.81	10.83	0.448	3.800
246.809	0.37450	31.05	29.23	0.00295	43.90	24.84	6.21	13.05	15.67	14.36	16.69	10.48	0.464	3.940
270.316	0.40350	31.48	29.90	0.0031	43.88	24.89	6.59	13.20	15.90	14.60	16.88	10.29	0.494	4.192
285.000	0.43200	31.39	29.90	0.0031	43.88	24.98	6.41	13.15	15.95	14.60	16.79	10.38	0.481	4.082
305.574	0.47140	31.44	29.93	0.00313	43.89	24.65	6.79	13.05	15.76	14.41	17.03	10.24	0.508	4.313
334.956	0.51390	31.53	30.12	0.00323	43.89	24.90	6.63	13.10	15.85	14.48	17.05	10.42	0.492	4.180
360.000	0.55930	31.53	30.12	0.00323	43.89	24.90	6.63	13.00	15.71	14.36	17.17	10.54	0.488	4.140
379.029	0.61620	31.30	29.93	0.00317	43.88	24.90	6.40	12.86	15.66	14.26	17.04	10.64	0.470	3.988

Table 5. Computed data for air flow rate of 685 CFM.

X Grains Frost ft^2	ΔP in H$_2$O @70°F	AIRSIDE t_{a1} °F	t_{w1} °F	W_1 lb/lb$_a$	$\overset{o}{m}_a$ lb/min	t_{a2} °F	Δt_a °F	ANTIFREEZE t_{r1} °F	t_{r2} °F	t_{r_m} °F	$t_{a_1}-t_{r_m}$	$t_{a_2}-t_{r_m}$	$R = \dfrac{t_{a_1}-t_{r_m}}{t_{a_2}-t_{r_m}}$	ln R	U
0	0.1169														
49.95	0.1300	33.15	32.05	0.00355	51.24	27.35	5.80	14.52	18.00	16.26	16.89	11.09	1.523	0.421	4.172
70.517	0.1723	30.87	30.53	0.00345	51.37	24.75	6.03	12.46	15.71	14.09	16.78	10.66	1.574	0.454	4.510
91.085	0.2027	32.76	30.50	0.00310	51.29	26.11	6.65	12.58	15.95	14.27	18.49	11.84	1.562	0.446	4.425
111.652	0.2167	32.75	30.30	0.0030	51.31	25.83	6.89	13.01	16.19	14.60	18.15	11.23	1.620	0.482	4.783
123.405	0.2307	32.67	30.15	0.00298	51.29	25.90	6.77	12.72	15.94	14.33	18.34	11.57	1.585	0.461	4.574
141.034	0.2507	32.50	30.13	0.0030	51.30	25.83	6.67	12.53	15.66	14.01	18.49	11.82	1.564	0.447	4.435
155.725	0.2697	32.59	30.15	0.00298	51.30	25.93	6.66	12.53	15.90	14.22	18.37	11.71	1.569	0.450	4.469
161.602	0.2837	32.44	30.15	0.00299	51.30	25.70	6.74	12.68	15.85	14.27	18.17	11.43	1.587	0.464	4.601
173,355	0.2876	33.05	30.63	0.00306	51.28	26.35	6.70	13.30	16.56	14.93	18.12	11.42	1.587	0.462	4.582
193.922	0.3281	32.5	30.58	0.00314	51.30	26.30	6.20	13.55	16.81	15.18	17.32	11.12	1.558	0.443	4.395
199.704	0.3546	32.54	30.58	0.00314	51.30	25.90	6.64	12.78	15.89	14.34	18.20	11.56	1.574	0.454	4.504
217.428	0.3795	32.50	30.58	0.00314	51.30	26.02	6.48	12.53	15.84	14.19	18.31	11.83	1.548	0.437	4.335
258.563	0.4534	32.44	30.63	0.00314	51.30	26.12	6.32	12.86	15.95	14.40	18.04	11.72	1.539	0.431	4.276

Table 6. Computed data for air flow rate of 775CFM.

$\frac{X}{\text{Grains Frost}}$ ft^2	ΔP in H_2O @ 70°F	AIRSIDE					Δt_a °F	ANTIFREEZE			$t_{a_1}-t_{r_m}$ °F	$t_{a_2}-t_{r_m}$ °F	$R = \dfrac{t_{a_1}-t_{r_m}}{t_{a_2}-t_{r_m}}$	$\ln R$	U Btu/hr-ft²-°F
		t_{a_1} °F	t_{w_1} °F	W_1 lb/lb$_a$	$\overset{\circ}{m}_a$ lb/min	t_{a_2} °F		t_{r_1} °F	t_{r_2} °F	t_{r_m} °F					
0	0.1448														
58.764	0.2197	31.48	28.90	0.00275	58.12	26.06	5.42	13.99	16.91	15.45	16.03	10.61	1.511	0.413	4.6421
70.517	0.2522	32.30	29.93	0.00293	58.07	26.12	6.18	12.67	15.95	14.31	17.99	11.81	1.523	0.421	4.7280
99.900	0.2991	32.30	30.30	0.00308	58.06	26.03	6.27	12.86	15.85	14.36	17.94	11.64	1.537	0.430	4.829
126.340	0.3490	32.72	30.72	0.00314	58.02	26.64	6.08	13.00	16.68	14.84	17.88	11.80	1.515	0.416	4.662
167.480	0.4415	32.0	30.45	0.00320	58.07	26.12	5.88	12.91	15.95	14.43	17.57	11.69	1.503	0.408	4.576
190.984	0.4684	31.92	30.30	0.00318	58.05	26.12	5.80	12.77	15.66	14.22	17.70	11.90	1.487	0.397	4.474